Nonstationary nonlinear effects in optical microspheres

Alexey E. Fomin and Michael L. Gorodetsky

Faculty of Physics, Moscow State University, 119992, Moscow, Russia

Ivan S. Grudinin

California Institute of Technology, 103-33, Pasadena, California 91125

Vladimir S. Ilchenko

Jet Propulsion Laboratory, California Institute of Technology, 4800 Oak Grove Dr., Pasadena, California 91109-8099

Received April 15, 2004; revised manuscript received September 2, 2004; accepted September 21, 2004

Thermal nonlinearity can produce oscillatory instability in optical microspheres. We experimentally demonstrate this instability and analyze the conditions needed to observe this regime. The observed behavior is in good agreement with the results of numerical simulation. In pure fused silica with low optical absorption the thermal oscillations are suppressed owing to an interaction of thermal and Kerr nonlinearities. We also describe experimentally observed slow and irreversible thermo-optical processes in microspheres. © 2005 Optical Society of America

OCIS codes: 190.3100, 190.4870, 190.1450.

1. INTRODUCTION

Optical microspheres with whispering gallery modes (WGMs) of total internal reflection[1] as well as their novel toroidal derivatives[2,3] uniquely combine submillimeter size with small volume-of-field localization ($V_{\text{eff}} \sim 10^{-9}\,\text{cm}^3$) and a very high quality factor. Even for such relatively linear material as fused silica, this combination provides the low threshold of optical bistability.[4] The threshold scales as V_{eff}/Q^2 (Q is an optical quality factor), and bistability can easily be seen at microwatts of optical power in fused-silica microspheres. This nonlinear effect may be either useful or undesirable, depending on application. In addition to fast Kerr nonlinearity, optical microspheres reveal slow thermal nonlinearity. Under the Kerr nonlinearity we understand the summary effect of cubic nonlinearities—electronic, strictional, and lattice unharmonicities, which are inseparable in many cases. Thermal nonlinearity results from a heating of mode volume by the power absorbed in a microsphere owing to nonzero optical losses. The value of thermal nonlinearity is not constant but depends on the rate of internal optical field intensity variations and therefore on the history and the rate of changes of difference between the resonator's eigenfrequency and input laser frequency. Generally speaking, thermal nonlinearity can be described by two characteristic times. The first describes thermal relaxation of the mode volume in the bulk of the microsphere, and the second is associated with the thermal relaxation of the microsphere as a whole.[5] In the same paper an interesting regime of oscillatory instability was observed. A similar example of the instability is presented in Fig. 1, which represents the nonlinear resonant curve as seen on the oscilloscope in experiments. Tentative explanation of this phenomenon, which was proposed in the aforementioned article,[5] required either two nonlinear mechanisms with different signs or two excited modes in the resonator. It is known, however, that the relaxation-type nonlinearity can produce oscillatory instability even in a single-mode resonator.[6] The first attempt to explain the oscillatory instabilities in microspheres with this approach was made by Belokopytov.[7] However, the quantitative estimates were significantly different from the experimental results.

Surprisingly, oscillatory and chaotic regimes that were sporadically observed in our early experiments were not observed in later experiments with microspheres in our group and were not observed in other laboratories afterwards. The obvious reason, as we recently realized was that in subsequent research the experiments were done with high-purity glasses in which the predominant mechanism of loss in the visible and near IR band was scattering and not absorption. Progress in our resonator fabrication technique allowed us[8] to reach the fundamental limit of $Q \sim 10^{10}$ at $\lambda = 0.63\ \mu$m. As the theoretical analysis below shows, if the absorption is small enough for the thermal-relaxation nonlinearity to be equal to the instant Kerr one, the competition of the two effects prevents the observation of the oscillatory instability. When we returned to fabrication of microspheres using the original, higher-absorption silica, we were able to reproduce the effect and study it in more detail.

2. OPTICAL NONLINEARITY IN MICROSPHERES

The wave equation for the electric field $\mathbf{E}_s$ in a sphere in first-order approximation has the following form:

Fig. 1. Nonlinear resonance and oscillatory instability in optical microsphere observed in the experiment. Horizontal axis corresponds to detuning from the resonant frequency; vertical, output intensity.

$$\Delta \mathbf{E}_s - \frac{\epsilon(\mathbf{r})}{c^2}\left(\frac{\partial^2 \mathbf{E}_s}{\partial t^2} + 2\delta\frac{\partial \mathbf{E}_s}{\partial t}\right) = \frac{4\pi}{c^2}\left[\frac{\partial^2 \mathbf{P}_p(\omega)}{\partial t^2} + \frac{\partial^2 \mathbf{P}_n(\omega)}{\partial t^2}\right], \quad (1)$$

where $\epsilon(\mathbf{r})$ is a linear dielectric constant of the medium (equal to the squared refractive index n^2 inside the sphere and unity outside) and $\delta = \delta_a + \delta_s + \delta_c$ describes total losses ($Q = \omega/2\delta$), taking into account internal absorption (δ_a), internal and external scattering (δ_s), and coupling losses (δ_c). The right part of the equation describes additional polarization due to the pumping and nonlinear effects, $\mathbf{P}_n = \chi_n \mathbf{E}_s$. Optical absorption of the energy stored in the mode of the resonator leads to a generation of heat. Owing to thermal dependence a change of temperature leads to a change of refractive index proportionally to the temperature shift: $\theta = T(\mathbf{r}) - T_0$. Since the eigenfrequencies of the microsphere depend on the refractive index, this leads to the thermal nonlinearity. Taking into account the instant Kerr and this thermal nonlinearity we can express χ as follows:

$$\chi_n = \frac{\epsilon}{2\pi}\beta\theta + \chi^{(3)}(\omega)E_s^2, \quad (2)$$

where $\beta = (1/n)(\partial n/\partial T)$ is the thermal dependence coefficient of refractive index. Using rotation wave approximation

$$\mathbf{E}(\mathbf{r}, t) = a(t)\mathbf{E}_0(\mathbf{r})\exp(i\omega t), \quad (3)$$

where $\mathbf{E}_0(\mathbf{r})$ describes the normalized field distribution of a chosen eigenmode of the unperturbed lossless microsphere,

$$\int |\mathbf{E}_0|^2 d\mathbf{r} = 1, \quad (4)$$

and $a(t)$ is a slowly varying amplitude, we multiply the wave equation by $\mathbf{E}_0^*(\mathbf{r})$ and integrate over the entire volume to obtain the first nonlinear differential equation for our analysis:

$$\dot{a} + a\left\{\delta + i\left[\Delta\omega + \frac{2\pi\omega_0\chi^{(3)}}{n^2 V_{\text{eff}}}|a|^2 + \omega_0\beta\Theta\right]\right\} = i\left(\frac{\pi\omega_0 W}{n^2 V_{\text{eff}} Q}\right)^{1/2}. \quad (5)$$

Here $\Delta\omega = \omega - \omega_0$ is the detuning of the pumping laser frequency from the unperturbed resonance eigenfrequency ω_0, W is the laser power, Θ is the average heating over the volume of the mode

$$\Theta = \int (T - T_0)|\mathbf{E}_0(\mathbf{r})|^2 d\mathbf{r}, \quad (6)$$

and V_{eff} is determined by the following simple formula:

$$V_{\text{eff}}^{-1} = \int |\mathbf{E}_0(\mathbf{r})|^4 d\mathbf{r}. \quad (7)$$

The definition of effective volume [Eq. (7)] is very useful and appears in the same form not only for the nonlinearity-related problems but also in analysis of scattering.[9] It is not difficult to understand; to find the effective volume one should average the intensity distribution over this distribution, hence the fourth power [see Eq. (4)]. This definition is more formal and is often more convenient than the alternative one: $\int |E_0|^2 dv = |E_0|^2_{\max} V_{\text{eff},m}$, especially for complex modes with many maxima. For the most localized $\text{TE}_{\ell\ell 1}$ mode in microspheres $V_{\text{eff}} \simeq 2V_{\text{eff},m} \simeq 3.9R^{11/6}(\lambda/n)^{7/6}$, where R is a microsphere's radius.

3. THERMAL EFFECT

To calculate the effect of thermal nonlinearity we start with the equation of thermal diffusion:

$$\frac{\partial T}{\partial t} - D\Delta T = \frac{n\alpha_a c}{4\pi C\rho}|\mathbf{E}|^2, \quad (8)$$

where $D = \lambda^*(\rho C)^{-1}$ is thermal diffusivity, λ^* is thermal conductivity, ρ is material density, C is a specific heat capacity of the material of the resonator, α_a is the part of the extinction coefficient corresponding to absorption, and c is the speed of light. Note that another component of losses—scattering—does not influence thermal nonlinearity. $|\mathbf{E}|^2 = I(t)|\mathbf{E}_0|^2$, where $I(t) = |a(t)|^2$ is intensity, varying slowly as compared with the optical relaxation time of the mode

$$\frac{1}{I}\frac{dI}{dt} \ll \frac{\omega_0}{Q}.$$

The energy density in the mode is $\mathcal{E}(t) = I(t)n^2/4\pi V_{\text{eff}}$.

The relaxation of the mode volume in the infinite media of microsphere may be found in spectral form, as follows:

$$T(t, \mathbf{r}) - T_0 = \frac{n\alpha_a c}{4\pi C\rho}\frac{1}{(2\pi)^4}\int\int \frac{I(\Omega)G(\mathbf{q})}{Dq^2 + i\Omega} \times \exp(i\Omega t + i\mathbf{q}\mathbf{r})d\Omega d\mathbf{q}, \quad (9)$$

where

$$G(\mathbf{q}) = \int |\mathbf{E}_0|^2 \exp(-i\mathbf{q}\mathbf{r})d\mathbf{r}. \quad (10)$$

The vector $\mathbf{q}$ here is the wave vector for the Fourier thermal waves in the medium, and Ω is the frequency of waves. In this approach thermal nonlinearity of the second kind, which is connected to the thermal relaxation of the microsphere itself, is lost. For a more rigorous analy-

sis, the decomposition into series of eigenfunctions, taking into account the boundary conditions, should be used. It is appropriate to note here that, for the microsphere 100 μm in diameter, the effective volume of the mode is nearly 3 orders of magnitude smaller than the total volume of the sphere; that is why the effects associated with the relaxation of the whole microsphere are significantly slower.[5]

We are interested in the value $\Theta(t)$, which is the average temperature difference over the volume of the mode:

$$\begin{aligned}\Theta(t) &= \int (T - T_0)|\mathbf{E}_0(\mathbf{r})|^2 d\mathbf{r} \\ &= \frac{n\alpha_a c}{4\pi C\rho}\frac{1}{(2\pi)^4}\int\int \frac{I(\Omega)|G(\mathbf{q})|^2}{Dq^2 + i\Omega}\exp(i\Omega t)d\mathbf{q}d\Omega \\ &= \frac{1}{2\pi}\int \Theta(\Omega)\exp(i\Omega t)d\Omega. \end{aligned} \tag{11}$$

We can formally obtain the following equation for $\Theta(\Omega)$:

$$i\Omega\Theta(\Omega) + \delta_\theta\Theta(\Omega) = \frac{n\alpha_a c}{4\pi C_\rho V_{\text{eff}}} I(\Omega), \tag{12}$$

where

$$\delta_\theta(\Omega) = \frac{D}{V_{\text{eff}}}\left[\int \frac{|G(\mathbf{q})|^2}{q^2 + i\Omega/D}\frac{d\mathbf{q}}{(2\pi)^3}\right]^{-1} - i\Omega. \tag{13}$$

Equation (13) is hard to use and evaluate. However, in the range of frequencies where $\delta(\Omega)$ depends weakly on Ω, a reasonable estimate may be obtained in most cases directly from (8): $\Delta\theta \sim -2\theta/b^2$, where b is the half-thickness of the mode in the direction of the largest field gradient, which is the radial direction for the microsphere. Hence,

$$\delta_\theta \simeq 2D/b^2, \tag{14}$$

and the second differential equation for analysis is

$$\frac{\partial\Theta}{\partial t} + \delta_\theta\Theta = \frac{n\alpha_a c}{4\pi C\rho V_{\text{eff}}}|a(t)|^2. \tag{15}$$

The value $1/\delta_\theta$ has physical meaning of the characteristic thermal relaxation time. Equations (5) and (13) lead to the nonlinear system of differential equations:

$$\begin{aligned}&\dot{u} + \delta u - [\Delta\omega + \mu(u^2 + v^2) + \omega_0\beta\Theta]v = 0, \\ &\dot{v} + \delta v + [\Delta\omega + \mu(u^2 + v^2) + \omega_0\beta\Theta]u = F, \\ &\dot{\Theta} + \delta_\theta\Theta = \frac{\nu\delta_\theta}{\omega_0\beta}(u^2 + v^2), \end{aligned} \tag{16}$$

where the complex amplitude $a(t)$ from Eq. (5) was replaced by the sum of real quadrature components:

$$a(t) = u(t) + iv(t) \tag{17}$$

and

$$\mu = \frac{2\pi\omega_0\chi^{(3)}}{n^2 V_{\text{eff}}}, \quad \nu = \frac{\omega_0\beta n\alpha_a c}{4\pi C\rho V_{\text{eff}}\delta_\theta}, \quad F = \left(\frac{\pi\omega_0 W}{n^2 V_{\text{eff}} Q}\right)^{1/2}. \tag{18}$$

The system of Eqs. (16) describes the dynamic behavior of a microresonator, taking into account nonlinear thermal effect and Kerr nonlinearity. The stationary solution of Eq. (16) is determined by the following cubic equation for the internal intensity $I_0 = |a_0|^2 = u^2 + v^2$:

$$\{\delta^2 + [\Delta\omega + (\mu + \nu)I_0]^2\}I_0 - F^2 = 0. \tag{19}$$

This equation describes the classical hysteretic response of the nonlinear resonator with two stable branches and one unstable branch. Intensity is maximal not at the resonance frequency but for the detuning $\Delta\omega = -(\mu + \nu)I_0$ produced by both Kerr and thermal effects. Nonlinear effects are pronounced, and hysteresis is observable if this detuning is significantly larger than the half-width δ of the linear resonant curve. Thermal nonlinearity dominates if $\nu > \mu$, that is,

$$\chi_\theta = \frac{n^3\alpha_a\beta c}{8\pi^2 C\rho\delta_\theta} > \chi^{(3)}. \tag{20}$$

However, this equation is not enough to describe the behavior of the resonator for time intervals smaller than $1/\delta_\theta$. Before going into analysis of dynamics of the system we must compare the absolute values of thermal and Kerr effects in microspheres. In fused silica $\rho = 2.2\,\text{g/cm}^3$, $C = 6.7\times10^6\,\text{erg/(gK)}$, ($\text{erg} = 10^{-7}\,\text{J}$), $\lambda^* = 1.4\times10^5\,\text{erg/(cm s K)}$, $D = 9.5\times10^{-3}\,\text{cm}^2/\text{s}$, $\beta = 1\times10^{-5}\,\text{K}^{-1}$. For the fundamental $\text{TE}_{\ell\ell1}$ mode in a microsphere of medium size (index $\ell \simeq 2\pi nR/\lambda = 1000$, wavelength $\lambda = 0.63\,\mu\text{m}$, $n = 1.46$, radius $R = 70\,\mu\text{m}$), radial width of the mode $b = 0.84R\ell^{-2/3} \simeq 0.6\,\mu\text{m}$. In this way we obtain from Eq. (14) $\delta_\theta \simeq 5\times10^6\,\text{s}^{-1}$. Fundamental absorption in fused silica for visible and near IR may be described[10] as

$$\alpha_a \simeq 1.1\times10^{-3}\left(\frac{\text{dB}}{\text{km}}\right)\exp\left(\frac{56\ \mu\text{m}}{\lambda}\right), \tag{21}$$

which leads to $\alpha_a \simeq 4\times10^{-6}\,\text{cm}^{-1}$. This ultimately small absorption leads to $\chi_\theta \simeq 4\times10^{-16}\,\text{esu}$, which is nearly 1 order of magnitude smaller than electronic $\chi^{(3)} \simeq 5\times10^{-15}\,\text{esu}$. However, the laboratory fused silica has impurities, leading to $\alpha_a \simeq 6\times10^{-4}\,\text{cm}^{-1}$ corresponding to $Q = 2\pi n/\alpha\lambda = 3\times10^8$, observed in early experiments, and $\chi_\theta \simeq 6\times10^{-14}\,\text{esu}$ will be more than 1 order larger than the Kerr nonlinearity. Therefore below we analyze two cases separately: the appearance of oscillatory instability due to thermal nonlinearity alone and what happens with this instability when the Kerr's nonlinearity appears.

4. NONLINEAR REGIMES

Dynamic behavior of the phase trajectories may be described by linearized equations obtained from Eq. (16) for the new set of small parameters

$$\xi = u - u_0, \quad \eta = v - v_0, \quad \zeta = \Theta - \Theta_0 \tag{22}$$

in the vicinity of equilibrium states (u_0, v_0, Θ_0):

$$\dot{\xi} = -(\delta - 2\mu u_0 v_0)\xi + (\Delta_n + 2\mu v_0^2)\eta + \omega_0 \beta v_0 \zeta,$$

$$\dot{\eta} = -(\Delta_n + 2\mu u_0^2)\xi - (\delta + 2\mu u_0 v_0)\eta - \omega_0 \beta u_0 \zeta,$$

$$\dot{\zeta} = 2\frac{\nu\delta_\theta}{\omega_0\beta}u_0\xi + 2\frac{\nu\delta_\theta}{\omega_0\beta}v_0\eta - \delta_\theta\zeta, \quad (23)$$

where $\Delta_n = \Delta\omega + (\nu + \mu)I_0$ is the stationary nonlinear detuning from resonance. The solutions of Eqs. (23) are determined by the roots of the characteristic equation:

$$\lambda^3 + (2\delta + \delta_\theta)\lambda^2 + [(\mu + \nu)(3\mu + \nu)I_0^2 + 2\Delta\omega(2\mu + \nu)I_0 + \Delta\omega^2 + \delta^2 + 2\delta\delta_\theta]\lambda + \delta_\theta[3(\mu + \nu)^2 I_0^2 + 4\Delta\omega(\mu + \nu)I_0 + \Delta\omega^2 + \delta^2] = 0. \quad (24)$$

From this algebraic equation, one may find the areas of stability for the system [Eq. (16)] using a Routh–Hurwitz criterion.[11] The number of positive roots, leading to instabilities, is determined by the number of sign changes in the sequence of $T_0 = a_0$, $T_1 = a_1$, $T_1T_2 = (a_2a_1 - a_3)T_1$, a_3, where a_0, a_1, a_2, and a_3 are the coefficients in the polynomial in λ [Eq. (24)] ($a_0 = 1$, $a_1 = 2\delta + \delta_\theta$, etc.). Because a_0 and a_1 are positive, the behavior of the system is determined by the sequence of roots of the two other terms T_2 and a_3:

$$I_{a3} = -[2\Delta\omega \pm (\Delta\omega^2 - 3\delta^2)^{1/2}] \times [3(\mu + \nu)]^{-1},$$

$$I_{T2} = \{-\Delta\omega(2\mu + \nu - \nu\delta_\theta/2\delta) \pm [\Delta\omega^2(\mu - \nu\delta_\theta/2\delta)^2 - (\delta + \delta_\theta)^2(\mu + \nu)(3\mu + \nu - \nu\delta_\theta/\delta)]^{1/2}\} \times [(\mu + \nu)(3\mu + \nu - \nu\delta_\theta/\delta)]^{-1}. \quad (25)$$

The first pair gives the borders of an unstable region of hysteretic resonance curve, which is not observable. The second pair shows the possibility of thermal oscillations, which are the main interest of this paper. These oscillations are possible if the interval determined by the second pair lies outside the borders determined by the first pair (Fig. 2).

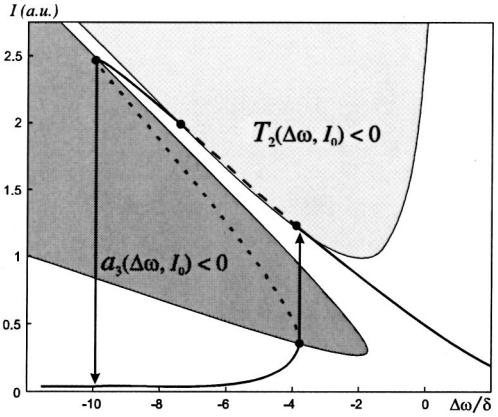

Fig. 2. Areas of stability for nonlinear resonance with relaxational nonlinearity. Dark-gray area marks the area of optical bistability; two stable states of output power are possible at given detuning. Dotted curve marks unstable state. Light-gray area shows the area of possible relaxational oscillations that can be observed on the dashed part of the nonlinear resonance curve.

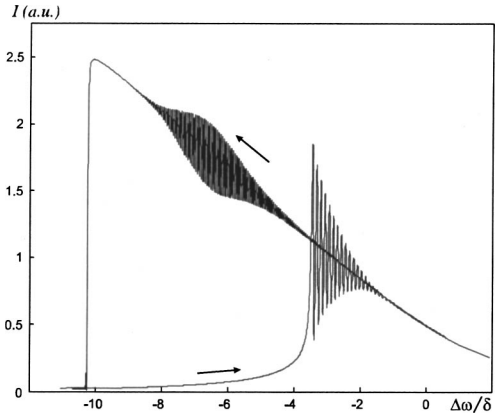

Fig. 3. Numerical simulation of WGM nonlinear optical resonance in microspheres with thermal nonlinearity: hysteretic response curve. In both optical and numerical experiments, the oscillatory behavior was observed on both branches of response curves.

The solutions [Eq. (25)] are greatly simplified in strong nonlinear regimes when νI_0, μI_0, $|\Delta\omega| \gg \delta$, δ_θ. In this case the zeros are given by three asymptotic straight lines: $I_{a3,1}(\mu + \nu) = -\Delta\omega/3$, $I_{a3,2}(\mu + \nu) = I_{T2,1}(\mu + \nu) = -\Delta\omega$, $I_{T2,2}(3\mu + \nu - \nu\delta_\theta/\delta) = -\Delta\omega$. The second asymptote coincides also with the asymptote for the maximum internal intensity I_0 for the nonlinear resonance curve. Thermal oscillations are possible only when $I_{T2,2} > I_{a3,2}$, i.e., $\nu > 2\mu\delta/\delta_\theta$:

$$\chi^{(3)} < \frac{\beta n^4}{8\pi^2 C\rho}\frac{\alpha_a}{\alpha_\Sigma} \simeq 4 \times 10^{-14}\frac{\alpha_a}{\alpha_\Sigma} \text{ esu}, \quad (26)$$

which means that the Kerr nonlinearity suppresses thermal oscillations in pure fused silica, where quality factor is determined mostly through scattering and $\alpha_a \ll \alpha_\Sigma$. Here $\alpha_\Sigma = \alpha_a + \alpha_{na} = 2\pi n/\lambda Q$ describes total losses in the microsphere, which include not only internal absorption but internal scattering and losses on surface inhomogeneities and in adsorbed surface layers, as well as additional losses due to the optical coupler. Substituting the value of $\chi^{(3)} = 5 \times 10^{-15}$ esu into Eq. (26) we obtain that the thermal oscillations are possible if $Q_a > 0.13Q$.

5. NUMERICAL MODELING

The numerical modeling of the dynamical behavior of the system described by Eqs. (16) was carried out in the MATLAB package for the experimentally determined, realistic set of parameters of microspheres. The Runge–Kutta method of fourth and fifth order was used. The obtained results of numerical modeling are in complete accordance with analytical calculations and are in agreement with observed experimental response curves. As clearly seen in Fig. 3 the oscillatory instability is observed on one of the slopes of the nonlinear resonant curve for a specific set of parameters.

Stable focus-type equilibrium state in the interval determined by zeroes of T_2 loses stability, and the soft

Andronov–Hopf bifurcation[12] with the ultimate cycle is formed (Fig. 4). For numerical and analytical evaluations the following parameters, the same as for Fig. 2, were used: input power 150 μW and microsphere diameter 100 μm, with TE WGM having $l - m = 20$; the modes of this order were typically excited in our experiments with limited laser scan range. Numerical experiments have also shown that when the Kerr nonlinearity obeys the condition in Eq. (26) the oscillations are not observed and the ultimate cycle turns into stable focus again. In experiments, however, the thermal oscillations dynamics sometimes resembled chaos. This behavior may be explained, as numerical modeling confirms, if the model of two or more neighboring optical modes is applied. In real microspheres each mode is a doublet owing to internal backscattering, which leads to the coexistence of two counterpropagating modes.[10] In this system the orbital cycle can become unstable (Fig. 5).

6. EXPERIMENTAL OBSERVATION OF THE OSCILLATIONS

In Fig. 6 one can see the scheme of the experimental setup. To observe the oscillations, we used small $2R \simeq 25$–160 μm fused-silica microspheres with quality factors of about $Q \simeq 10^7$–10^8, manufactured with the hydrogen–oxygen miniature torch. To avoid degradation of the Q factor owing to adsorption of atmospheric water, we placed microspheres upon fabrication into the special

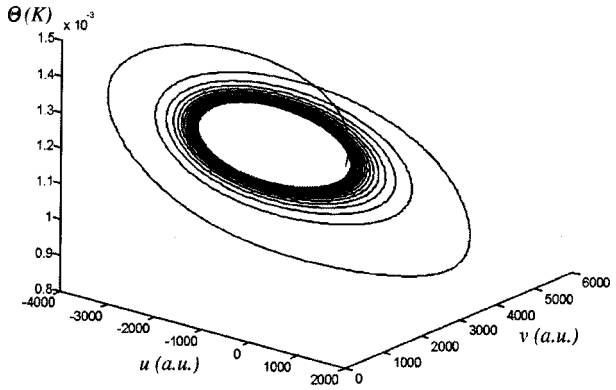

Fig. 4. Numerical simulation of WGM nonlinear optical resonance in microspheres with thermal nonlinearity—phase diagram.

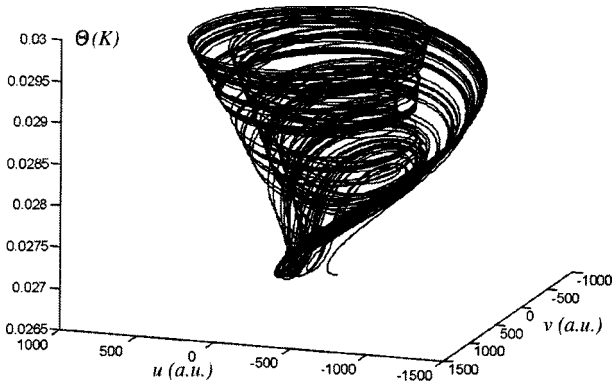

Fig. 5. Numerical simulation of chaotic regime in microsphere with thermal nonlinearity and two close optical modes.

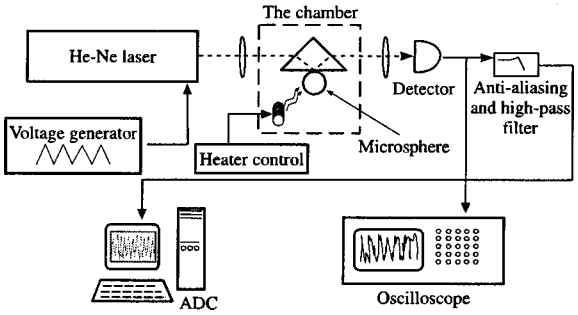

Fig. 6. Scheme of the experimental setup.

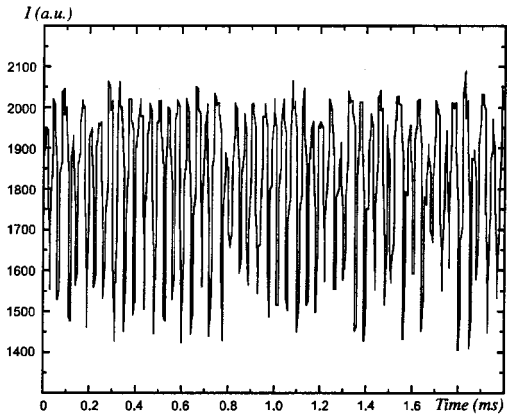

Fig. 7. Thermal nonlinearity and oscillations in the microsphere 82.5 μm in diameter. The picture represents thermal oscillations on the fraction of the slope of the nonlinear resonant curve shown in Fig. 8.

chamber where all measurements were carried out. The chamber was filled with dry, clean nitrogen. WGMs were excited in microspheres with a prism coupler with a He–Ne laser ($\lambda = 0.63$ μm) with a piezodriven front mirror. Laser frequency could be tuned within the range of approximately 0.7 GHz. The laser's maximum output power was ~540 μW. To measure the quality factor, we decreased the power fed into the microspheres with neutral glass filters to weaken thermal and Kerr nonlinearities.

A nichrome (nickel–chrome alloy) filament heater was placed near the resonator and used for coarse tuning of resonator eigenfrequency in the range of ~30 GHz. Narrow-range laser frequency sweeping (in the range of 700 MHz) was carried out through application of the ramp voltage to the piezoactuator of the laser mirror. This voltage produced a sweeping of the light frequency and allowed us to observe the resonant curves on the screen of the oscilloscope. The signal from the detector was observed with a digital oscilloscope and could be sampled with an analog-to-digital converter computer board.

In this research the intentional search and observation of the oscillations in the WGM was carried out. Instead of using the pure fiber-grade glasses similar to those used in the majority of recent experiments, we fabricated the microspheres using the original technical grade (96%) silica, which had increased absorption and yielded pronounced thermal nonlinearity of the WGMs. Low grade

of this silica was confirmed by a reduced melting temperature and by its increased luminance in a molten state.

Figure 8 depicts the thermorefractive oscillations observed in the microsphere with a diameter of 82.5 μm, which had the smallest effective mode volume among the several tested spheres. This picture presents the superimposed resonant curves obtained by a scanning of the laser frequency in two opposite directions in the vicinity of a WGM. For this, a triangular ramp voltage was applied to the piezoactuator of the laser mirror. The hysteretic feature due to nonlinearity can be easily observed, as well as the thermal oscillations on the slope of the nonlinear resonant curve. The curve is slightly tilted owing to the high-pass filter used in the setup to get rid of the constant offset. The oscillating mode has indices $l = 2\pi Rn/\lambda \simeq 600$, $l - m = 6 \pm 2$, as calculated from the observations of the WGM belt. This belt is caused by a scattering of light by the surface roughness and the dust of the microsphere. Oscillations were observed with 540 μW of pump power, as measured before the objective lens preceding the chamber with the microsphere. The results of observation are presented in Figs. 7 and 8. The measured Q factor of the mode, inferred at reduced pump power in the linear regime, was 7×10^8. The oscillations observed with the sweep turned off were close to the harmonic ones with a dominating spectral peak at 26 kHz, accompanied by numerous smaller harmonics and the background of a continuous spectrum.

In the microsphere with a diameter of 90 μm maximal coupling provided for 30% of 540 μW of pump power to be dissipated by the WGM. The oscillations were observed down to 20 μW (4%) of coupling and disappeared when coupling was reduced (through an increase of the prism gap) to ~10 μW of optical power going into the microsphere. They also disappear with a decrease of the Q factor (which may happen owing to a gradual contamination of the microsphere surface) and with a decrease of the gap between the microsphere and the prism coupler (a decrease of loaded Q). A characteristic frequency of these oscillations was 7 kHz, with harmonics at 14 and 21 kHz. The spectrum was continuous, and the width of these harmonics was of the order of several kilohertz. All of these effects were reproducible in our numerical model with approximately the same set of parameters as in experiment. We identify this oscillatory behavior mainly as the result of nonstationary and chaotic effects in the system with more than one optical mode (usually doublets) in presence of thermal nonlinearity. This possibility was confirmed by numerical simulations (see Section 5). Direct quantitative comparison, however, was not possible owing to some uncertainty in the estimate of the actual power absorbed in the resonator and the value of the coefficient of absorption, which could not be measured directly in our experiments, as the quality factor provides only the value of the sum of internal scattering, absorption, and surface losses.

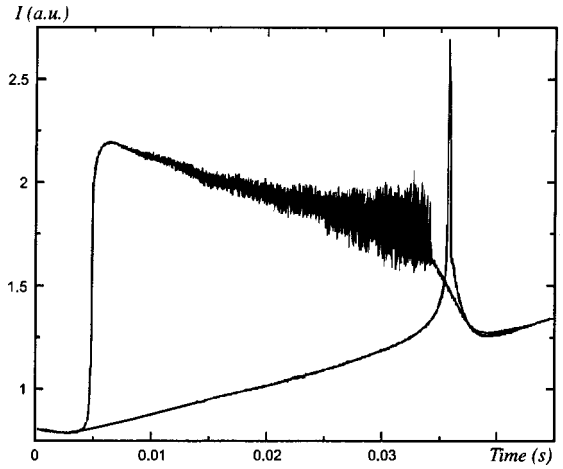

Fig. 8. Thermal nonlinearity and oscillations in the microsphere 82.5 μm in diameter. Sweep rate is 2.9 GHz/s.

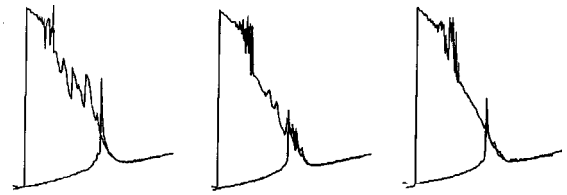

Fig. 9. Nonstationary thermal effects and bifurcations in the microsphere with the diameter 90 μm, $Q \simeq 10^8$. The oscillating area is to the top of the curve. Several accompanying peaks in the picture to the left are moving "down the resonant curve" and disappear later, as seen on the picture to the right.

The onset of oscillations in this resonator was preceded by a specific nonstationary process. This process emerges every time the nonlinearity is strong and power consumption in a mode is sufficiently high. The process can be observed when the frequency sweep is on, and one can see the dynamically refreshing resonant curve on the screen of the oscilloscope. Typical parameters accompanying the onset of the process are ~100 μW of power consumption in the mode, $Q \simeq 10^8$, and a nonlinearity-induced widening of the resonant curve above 100 MHz. The process itself looks like a splitting of the WGM or, in other words, an emergence of satellite resonant frequencies that change dynamically and irreversibly. Initially, the ordinary highly nonlinear resonant curve can be seen on the screen. Then from the point of the greatest energy consumption the second peak emerges, then another. These peaks are moving "down the resonant curve"; there can be several such moving peaks. Sometimes the oscillations emerge with one of these peaks, and the oscillating area also moves "down the slope" until it stabilizes on the slope of the resonant curve. This sequence is represented on the following series in Fig. 9, where one can see the superimposed resonant curves obtained by a scanning of the laser frequency in two opposite directions in the vicinity of the WGM. The entire process takes a few minutes or less; the time scale depends on the optical pump power.

We have observed inconclusive evidence of small but significant irreversible changes of the mode-quality factors in the case of the oscillatory process under consideration. These changes also lead to a degradation of oscillations when a certain power threshold is reached. When the oscillations were observed and digitized without the frequency sweep, they disappeared within 15 s, and when the frequency sweep was restored we found three new modes (triplet) in place of the original mode. After a few

minutes oscillations were resurrected, and these three modes merged into a single nonlinear mode, but its Q factor dropped significantly (about 2–5 times). We may suggest that the process of oscillation causes some degradation of material. The absorption of optical power may be not homogeneous inside the contaminated fused silica but connected with small loss centers. Large thermal pulsations of these heated centers with relatively high frequency could produce defects in the material of the microsphere analogous to "hole burning" that lead to increased losses owing to additional scattering. These local defects may partially "heal" after some time. Collapse and channeling of WGM owing to self-focusing produced by thermal nonlinearity again accompanied by large local heating and appearance of defects may be also considered. The described nonstationary and irreversible effects have also been observed in experiments with other microspheres. However, detailed study of the phenomena should be the subject of separate experiments that go beyond the scope of the current paper.

7. CONCLUSION

We have presented the theoretical analysis of the effects in microspheres associated with concurrence of Kerr and thermal nonlinearities. The main features of the experimentally observed oscillations are well captured by the analysis and are in agreement with the presented experimental results.

We observed experimentally and described qualitatively and quantitatively an interesting effect of thermal oscillations and bifurcations in optical microspheres as well as unusual irreversible processes at microwatt level of optical power. These effects, which may be undesirable in future applications of microspheres, generally disappear if modern high-grade quality materials are used.

ACKNOWLEDGMENTS

This work was supported by the President of the Russian Federation grant for young scientists MD-208.2003.02 and grant NS-1318.2003.2.

I. S. Grudinin's e-mail address is grudinin@caltech.edu.

REFERENCES

1. V. B. Braginsky, M. L. Gorodetsky, and V. S. Ilchenko, "Quality-factor and nonlinear properties of optical whispering-gallery modes," Phys. Lett. A **137**, 393–397 (1989).
2. V. S. Ilchenko, M. L. Gorodetsky, X. S. Yao, and L. Maleki, "Microtorus: a high-finesse microcavity with whispering-gallery modes," Opt. Lett. **26**, 256–258 (2001).
3. D. K. Armani, T. J. Kippenberg, S. M. Spillane, and K. J. Vahala, "Ultra-high-Q toroid microcavity on a chip," Nature **421**, 925–928 (2003).
4. H. M. Gibbs, *Optical Bistability: Controlling Light with Light* (Academic, New York, 1985).
5. M. L. Gorodetsky and V. S. Ilchenko, "Thermal nonlinear effects in optical whispering-gallery microresonators," Laser Phys. **2**, 1004–1009 (1992).
6. A. E. Salomonovich, "Automodulation at ferroresonance," Zh. Tekh. Fiz. **22**, 245–258 (1952) (in Russian).
7. G. V. Belokopytov, "Electrothermal instability of oscillations in temperature sensitive resonant systems," Vestn. Mosk. Univ., Ser. 3: Fiz., Astron. **3**, 11–15 (1997).
8. M. L. Gorodetsky, A. A. Savchenkov, and V. S. Ilchenko, "On the ultimate Q of optical microsphere resonators," Opt. Lett. **21**, 453–455 (1996).
9. M. L. Gorodetsky, A. D. Pryamikov, and V. S. Ilchenko, "Rayleigh scattering in high-Q microspheres," J. Opt. Soc. Am. B **17**, 1051–1057 (2000).
10. M. E. Lines, "Scattering losses in optic fiber materials. I. A new parametrization. II. Numerical estimates," J. Appl. Phys. **55**, 4052–4063 (1984).
11. G. A. Korn and T. M. Korn, *Mathematical Handbook for Scientists and Engineers*, 2nd ed. (McGraw-Hill, New York, 1968), p. 17.
12. Yu. A. Kuznetsov, *Elements of Applied Bifurcation Theory*, 2nd ed. (Springer-Verlag, New York, 1998), p. 135.